LA-2468

C.3

LOS ALAMOS SCIENTIFIC LABORATORY
OF THE UNIVERSITY OF CALIFORNIA ○ LOS ALAMOS   NEW MEXICO

DOSIMETRY FOR THE LITTLE EVA CRITICAL ASSEMBLY

NEUTRON FLUX, SPECTRUM, AND TISSUE DOSE EVALUATIONS

LEGAL NOTICE

LOS ALAMOS SCIENTIFIC LABORATORY
OF THE UNIVERSITY OF CALIFORNIA   LOS ALAMOS   NEW MEXICO

DOSIMETRY FOR THE LITTLE EVA CRITICAL ASSEMBLY
NEUTRON FLUX, SPECTRUM, AND TISSUE DOSE EVALUATIONS

by

J. A. Sayeg
D. G. Ott
P. S. Harris

ABSTRACT

The leakage neutron flux and spectrum and the neutron and gamma dose versus distance relations were determined for the Little Eva critical assembly. These measurements were accomplished with the threshold detectors Pu^{239}, Np^{237}, U^{238}, and S^{32} for the evaluation of fast neutron flux, spectrum, and neutron tissue dose; and bare and cadmium covered gold foils were used for the evaluation of the thermal flux. The gamma dose was determined with tetrachloroethylene chemical dosimeters. These measurements show this assembly to have the lowest gamma to neutron dose ratio of any assembly tested to date.

ACKNOWLEDGMENTS

-2-

CONTENTS

ILLUSTRATIONS

CHAPTER 1

INTRODUCTION

The purpose of the present investigation was to provide a calibration of the leakage neutron flux and neutron and gamma tissue doses as a function of distance for the Little Eva critical assembly.

CHAPTER 2

MATERIALS AND METHODS

2.1 Description of Little Eva

The Little Eva critical assembly consists of a pseudo-
sphere arrangement of U^{235} (approximately 22 kg) mounted on
the table of a drill press (1). The critical mass consists
of 1/2 in. cubes surrounded by tuballoy (U^{238}) tamper. The
exterior dimensions of the tuballoy tamper are approximately
that of a cube 8-1/2 in. on a side. The coarse control is
obtained by varying the relative amounts of tamper and active
material. The fine control of the assembly is a 2 in. cubic
block of tuballoy which can be moved in or out from the
critical arrangement of U^{235} by a small motor and gear system.
The assembly is mounted in the corner of a trailer (see
Fig. 1). A cab houses the control cables necessary for re-
mote operation (Fig. 2). The cab control and reactor trailer
can be separated by approximately 1/4 mile during operation.
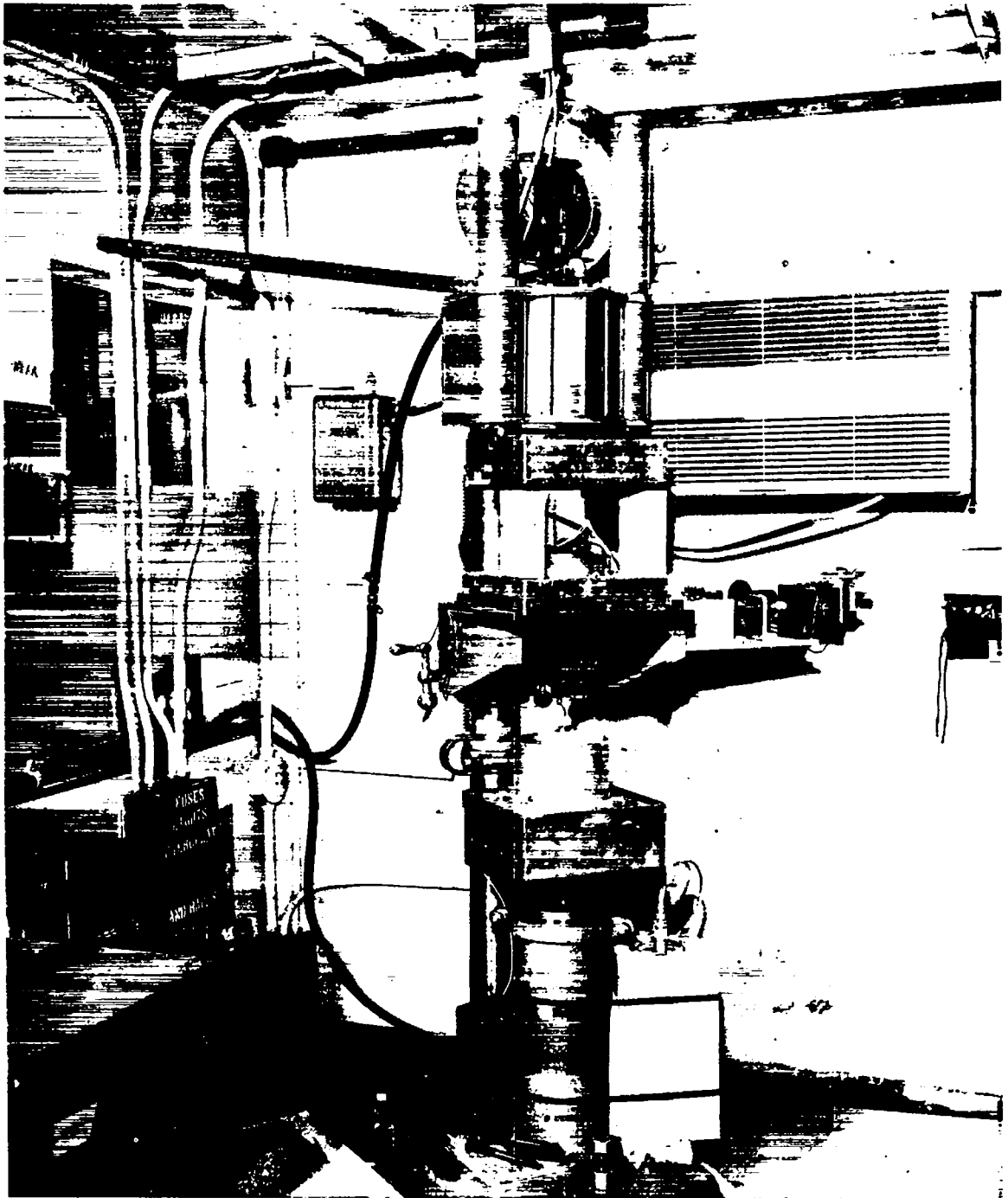
Fig. 1.   Little Eva critical assembly set-up in trailer.
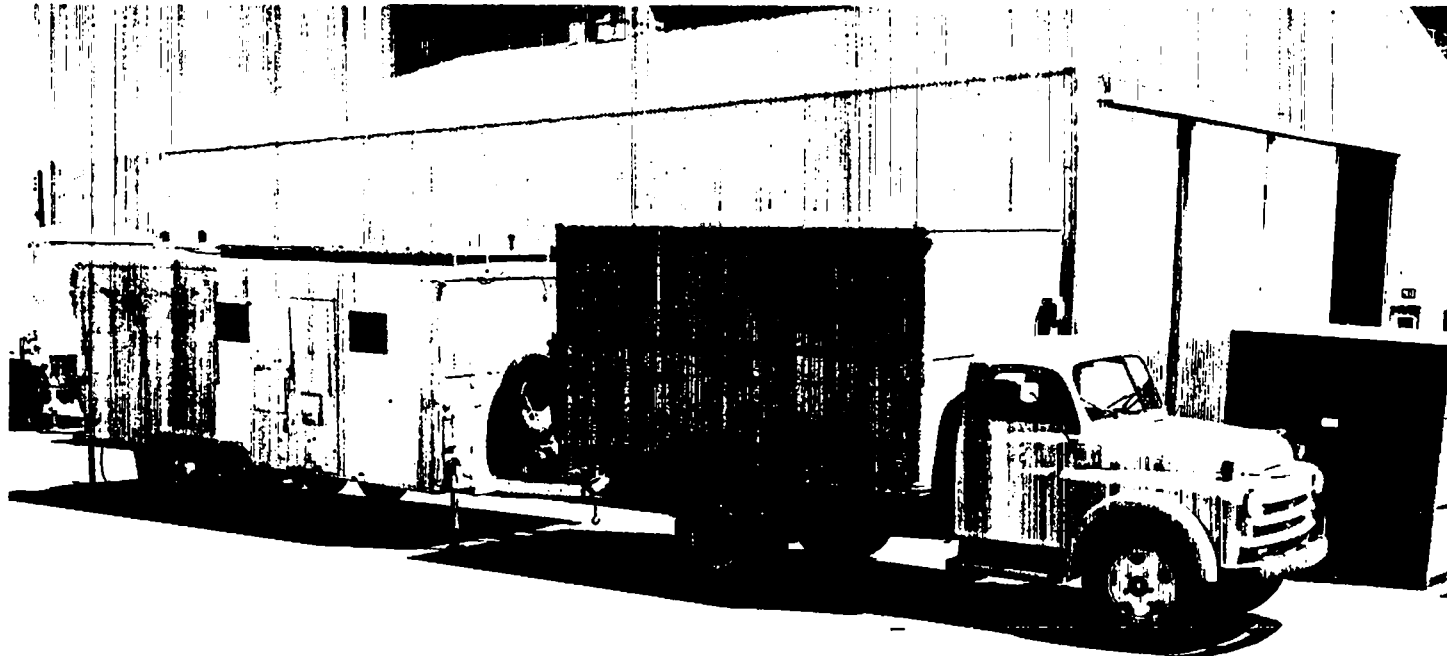
Fig. 2.   Truck and trailer used for transporting Little Eva critical assembly.

2.2 Neutron Dosimetry

2.2.1 Neutron Flux Measurements

The method of Hurst and his co-workers (2-4) was used for the measurement of fast and thermal neutron fluxes. The threshold detectors Pu^{239} (surrounded by 2 cm of B^{10}), Np^{237}, U^{238}, and S^{32} were used to measure neutron fluxes above the following threshold energies:

$$Pu^{239} \text{ (with 2 cm of } B^{10}) \qquad 0.004 \text{ Mev}$$
$$Np^{237} \qquad 0.75 \text{ Mev}$$
$$U^{238} \qquad 1.5 \text{ Mev}$$
$$S^{32} \qquad 2.5 \text{ Mev}$$

The foils Pu^{239}, Np^{237}, and U^{238} were 3/4 in. in diameter, copper canned, and varied in mass from 0.10 to 3.0 g. The S^{32} foils were 1-1/2 in. in diameter and 3/8 in. thick and weighed 20 g.

To facilitate handling, the fission foils Pu^{239}, Np^{237}, and U^{238} were placed in steel spheres containing 2 cm of B^{10}. The foils were surrounded by cadmium, which served to absorb any thermal neutrons reaching the foil area.

The thermal neutron flux ($E_n < 0.5$ ev) was estimated by bare and cadmium difference measurements of gold foil activation. The gold foils used were 1/2 in. in diameter and 0.010 in. thick.

The sulfur and bare and cadmium covered gold foils were
placed in a separate holder constructed of Dural. The holder
was approximately 8 in. long, 2 in. wide, and 3/8 in. thick.
The sulfur foil was centered in the holder with gold foils
at each end. The bare and cadmium covered gold foils were
separated by approximately 6 in.

Fission foil gamma ray activities were measured using
a scintillation counter (Fig. 3). The foil was placed between
2 opposing RCA No. 6655 phototubes with 1-3/4 in. diameter,
1-1/2 in. thick, thallium activated, sodium iodide crystals.
A 1/4 in. thick lead absorber was interposed between each
crystal and the foil to reduce the natural background activity
of the foil. The outputs of the phototubes were connected to
a Model 250N preamplifier, thence to a Model 250 amplifier,
a Model 120 dual channel analyzer, and finally to 2 Model 775
scalers (see Fig. 3). These electronic components provided a
means of counting gamma rays simultaneously above two different
threshold bias levels. The bias levels chosen were 0.51 and
1.2 Mev. The phototubes were balanced by adjusting the voltage
on each tube. The voltage divider and balancing circuits are
shown in Fig. 4.

The counting system was calibrated according to the most
recent procedures adopted by the Oak Ridge group (4). Equiv-
alent fission foils of Pu^{239}, Np^{237}, and U^{238} were fabricated

LEAD ABSORBER

SODIUM IODIDE CRYSTAL

PHOTOTUBE

THRESHOLD FOIL
DETECTOR

LEAD ABSORBER

SODIUM IODIDE CRYSTAL

PHOTOTUBE

TUBE SHIELD

H.V. TUBE #1

H.V. TUBE #2

SIGNAL-TUBE #1

VOLTAGE
CONTROL
BOX

POWER
SUPPLY

SIGNAL-TUBE #2

MODEL 250N
PREAMPLIFIER

MODEL 250
AMPLIFIER

VOLTAGE
REGULATOR

110 VOLTS

MODEL 120
DUAL ANALYZER

MODEL 775
SCALER

MODEL 13
ELECTRONIC TIMER

MODEL 775
SCALER

Fig. 3.   The dual scintillation counting shield K-2 and
associated electronics.
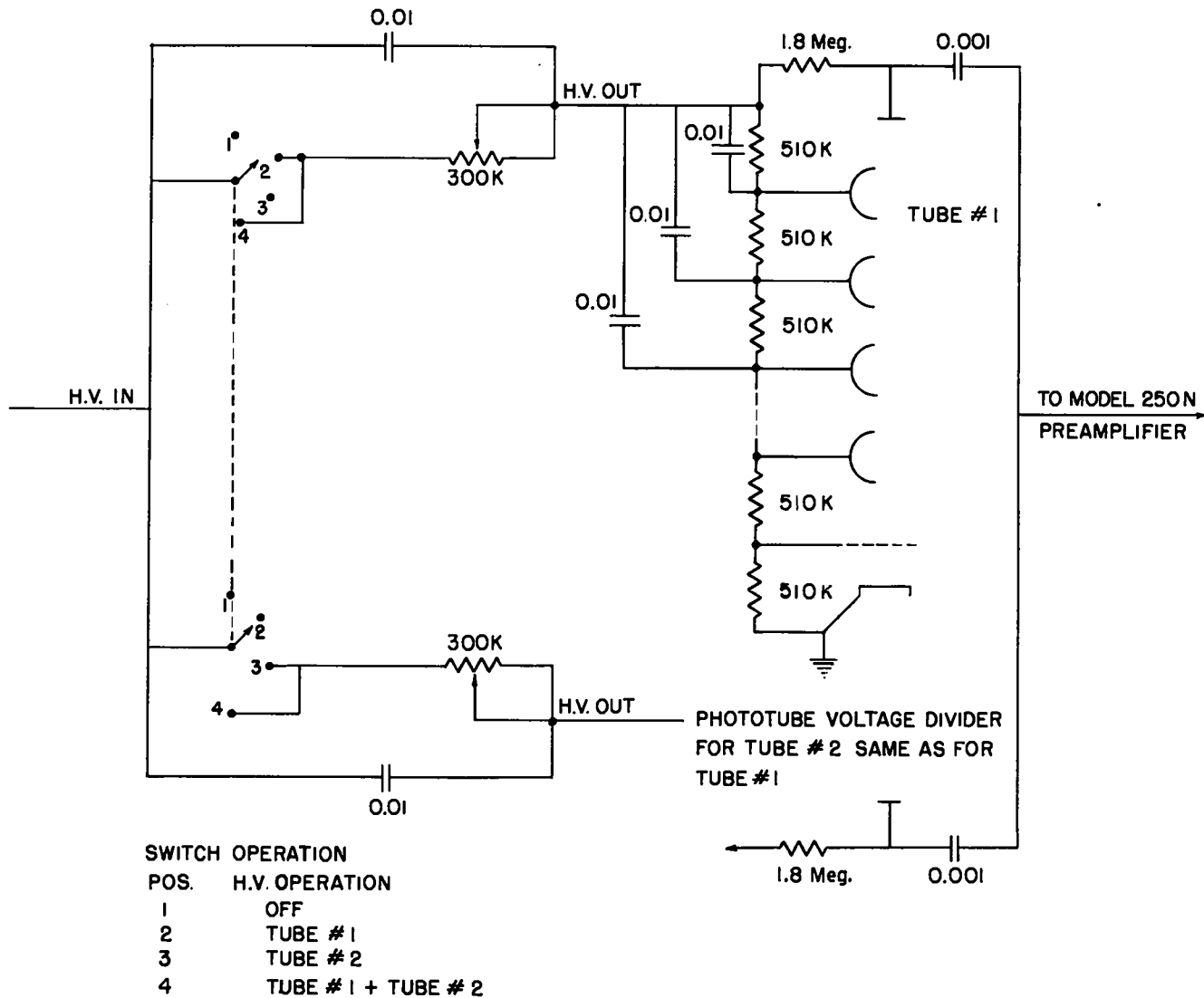
Fig. 4.   The voltage divider and balancing circuits used with the counting shield K-2.

from Pu^{239} and U^{235}. The composition of each foil is shown in Table 1. The foils were plated on a 10 mil nickel backing and surrounded by 5 mils of copper. The over-all dimensions of the foils were approximately 0.02 in. in thickness and 3/4 in. in diameter. Blank foils containing the nickel backing and copper can covering were also fabricated to serve as controls for extraneous activity not produced by fission when exposed to thermal neutrons for calibration. To evaluate the self-shielding and flux depression effect of these foils, 2 Au^{197} foils 0.0005 in. thick and 1/2 in. in diameter were pasted on the surfaces with a small amount of Vaseline. The activity per unit mass of these thin Au^{197} foils was then compared to a similar Au^{197} foil exposed with no fission foil present. The factor was evaluated to be 1.07.

The fission foils were exposed to approximately 3×10^{11} thermal neutrons/cm^2 (10 per cent uncertainty). The decay curves are shown in Fig. 5. All measured fission activities were normalized to 3 hours post irradiation time. These "ratio curves" are shown in Fig. 6, with the evaluated calibration constants shown in Table 2. The cross sections used to evaluate the calibration constants are shown in Table 3 and are discussed in detail in Refs. 5 and 6. For flux evaluations, all measured fission gamma activities were also normalized to the 3 hour post irradiation time using the data in Fig. 6.

TABLE 1. FOIL MASS DATA FOR CALIBRATION OF THE DUAL COUNTING SHIELD K-2

Foil No.	Mass Pu^{239}, mg	Mass U^{235}, mg	Ratio $\dfrac{Pu^{239}}{U^{235}}$	Equivalent Mass Pu^{239}, mg
P-2	10.1	--	--	10.1
N-2	5.2	7.0	0.74	10.4
U-2	8.6	4.0	2.15	11.6

TABLE 2. THREE HOUR CALIBRATION CONSTANTS FOR THE DUAL COUNTING SHIELD K-2

Gamma Ray Counter Energy Bias, Mev	Counter Calibration Constant K, $n/cm^2/c/m/g$		
	K_{Pu}	K_{Np}	K_U
0.51	4.60×10^6	--	1.55×10^7
1.2	2.25×10^7	1.93×10^7	7.40×10^7

TABLE 3. EFFECTIVE CROSS SECTIONS IN B^{10} SPHERES* WEIGHTED FOR DIFFERENT FISSION SPECTRA

Foil Type	$(\sigma_{eff})_{weighted}$, barns	
	Godiva Spectrum**	Fission Spectrum**
Pu^{239}	1.78	1.80
Np^{237}	1.71	1.66
U^{238}	0.55	0.53

*For a 2 cm B^{10} sphere of 1.1 g/cm^3 density.

**Both spectra were extrapolated from 200 to 0 kev (6) in these evaluations.
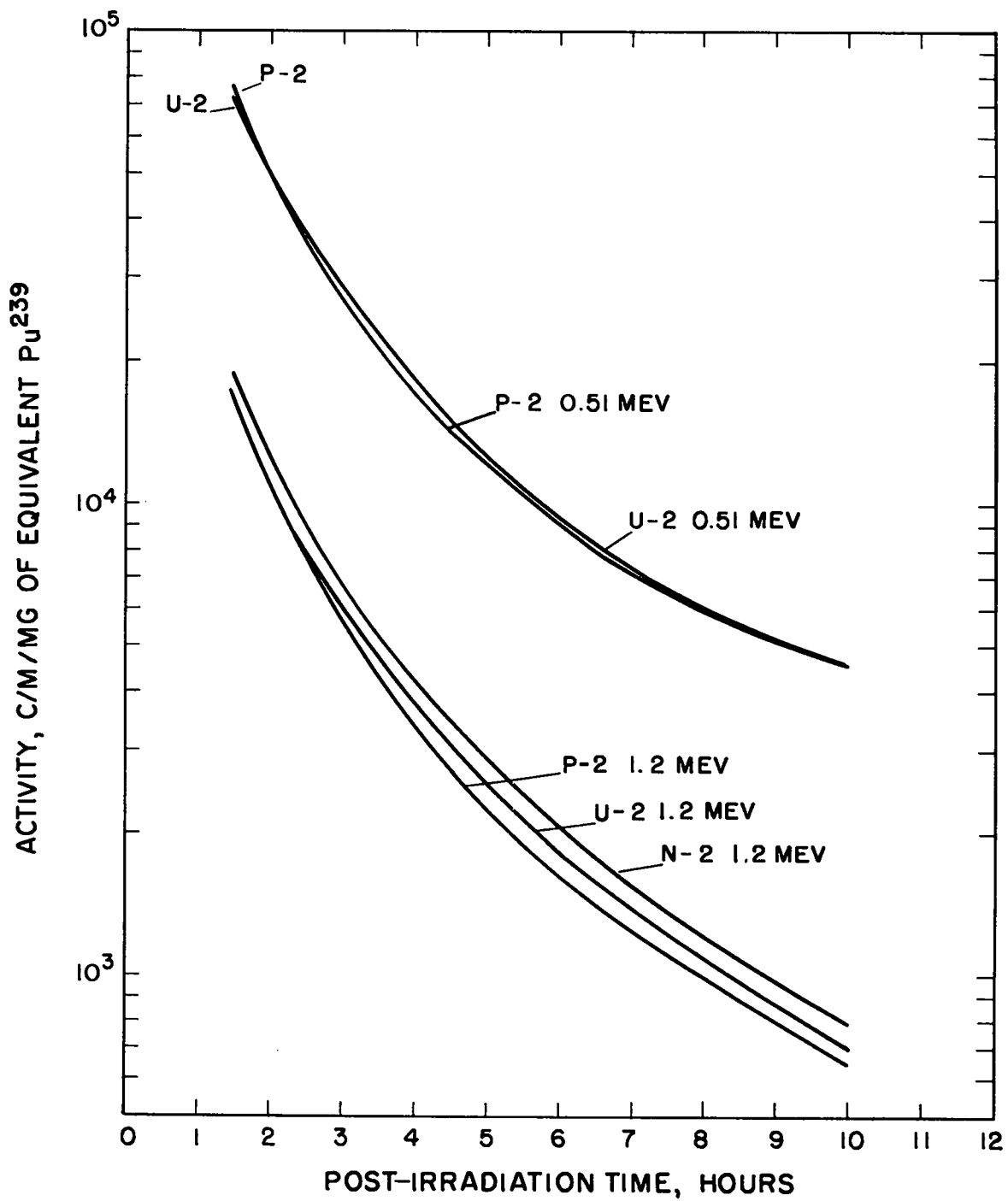
Fig. 5.   Decay curves for equivalent foils of Pu^{239} (P-2),
Np^{237} (N-2), and U^{238} (U-2).
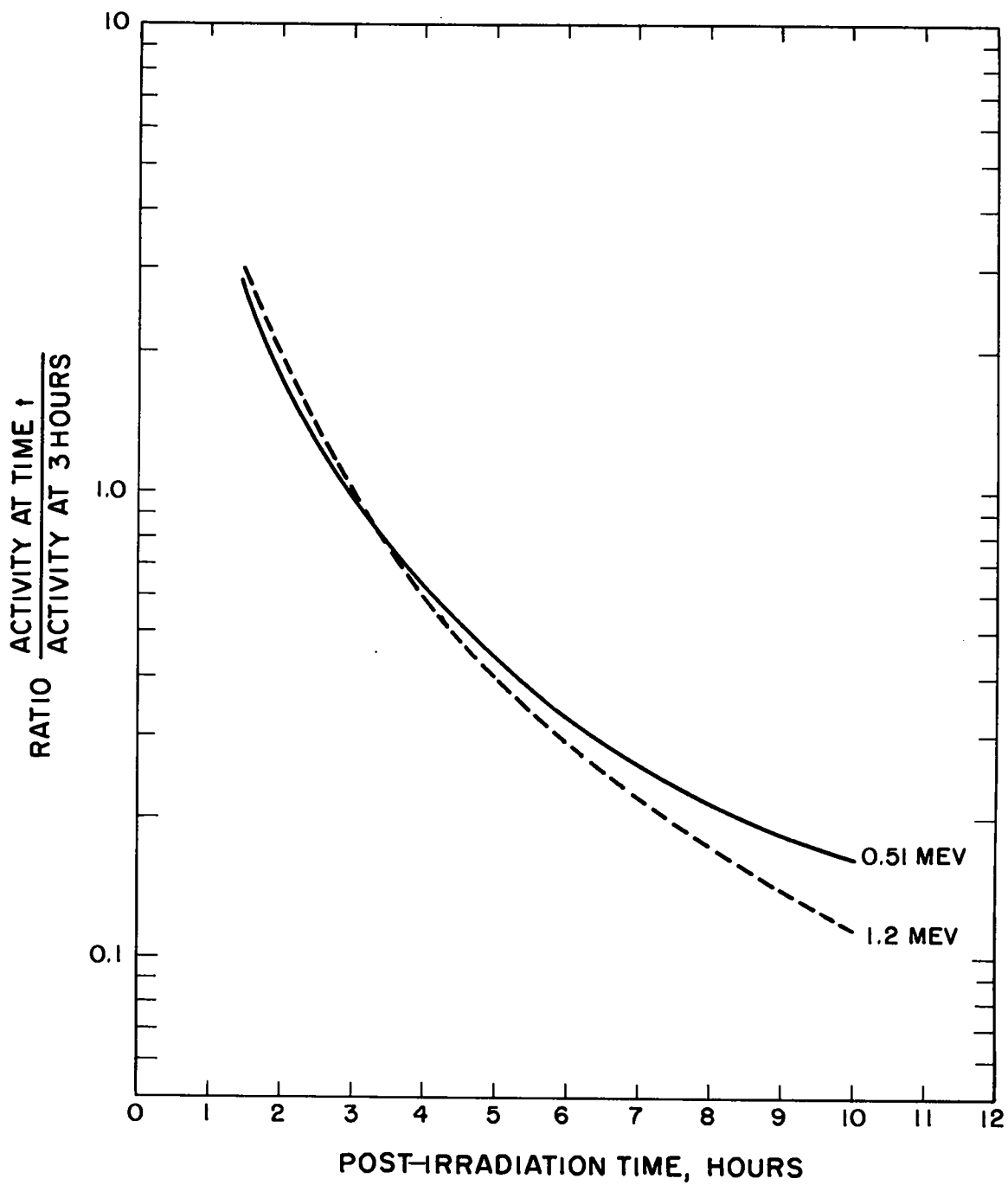
Fig. 6. Plutonium[239] ratio curves normalized to 3 hours post irradiation time.

Usually five 1 minute counts were taken for each exposed foil. The counting time of each foil was spaced by approximately 1/2 hour.

2.2.2 Sulfur Pellet Beta Counter

The P^{32} induced activity in the sulfur pellet was measured using a 2 in. diameter, 5/32 in. thick, plastic scintillator covered with 0.002 in. of aluminum foil and connected to an RCA No. 6655 phototube. The output of the phototube was connected to an amplifier and scaler. The counter was intercalibrated against the HRL plastic beta scintillation counter (5). It had a calibration constant of 1.22×10^7 $n/cm^2/c/m$ (initial counting rate) for a standard pellet (corrected for the change in cross section from the 14 Mev reference energy to the 2.5 Mev effective threshold, assuming a fission spectrum).

2.2.3 Gold (Au^{198}) Gamma Counter

The induced activity in Au^{198} was measured using a 1-3/4 in. diameter, 1-1/2 in. thick, thallium activated, sodium iodide crystal connected to an RCA No. 6655 phototube, amplifier, and scaler. A 1/16 in. aluminum absorber (400 mg/cm^2) was interposed between the crystal and foil to eliminate any Au^{198} beta ray activity. The counter was

intercalibrated against the HRL standard gold gamma counter (5). The gold counter used had a calibration constant of 2.16 x 10^5 n/cm^2/c/m (initial counting rate) for a standard gold disc of 0.66 g.

2.2.4 Tissue Dose Evaluations

The neutron tissue dose (single collision) due to fast neutrons was calculated from the following formula, developed semi-empirically (6):

$$D_T = 1.28 \times 10^{-9}(F_{Pu} - F_{Np}) + 2.46 \times 10^{-9}(F_{Np} - F_U)$$

$$+ 2.97 \times 10^{-9}(F_U - F_S) + 3.84 \times 10^{-9}(F_S) \qquad \text{(Eq. 1)}$$

where D_T = fast neutron tissue dose, rads

F_{Pu} = integral fast neutron flux measured by Pu^{239}, n/cm^2

F_{Np} = integral fast neutron flux measured by Np^{237}, n/cm^2

F_U = integral fast neutron flux measured by U^{238}, n/cm^2

F_S = integral fast neutron flux measured by S^{32}, n/cm^2

The coefficient before each parenthesis represents the average single collision tissue dose for the energy interval under consideration (i.e., between the thresholds of the detectors noted).

The thermal neutron tissue dose was estimated for a small biological object (20 to 30 g) by applying the conversion factor 5 x 10^{-11} rad/n/cm^2.

2.3 Gamma Dose Measurements

The dose from the gamma component was measured using the chemical dosimeter system which has been described previously (7). Briefly, it is composed of tetrachloroethylene overlayered with an aqueous pH indicator solution and contained in sealed 1 ml glass ampules. Gamma radiation induces a chemical chain reaction in the tetrachloroethylene which results in the production of acid. The amount of acid produced is directly proportional to the dose and is determined by spectrophotometric evaluation of the color changes produced in the indicator solution.

These dosimeters have a measurable response to fast neutrons which becomes quite important at high neutron to gamma ratios. One hundred rads of fast neutrons produces the same amount of acid as 4 roentgens of gamma radiation. The gamma dose, D_γ, in a mixed radiation field is thus

$$D_\gamma = R - 0.04 \, D_N \qquad \text{(Eq. 2)}$$

where R is the dosimeter response in gamma equivalent roentgens, and D_N is the tissue dose of fast neutrons in rads.

Response to thermal neutrons is eliminated by shielding the gamma dosimeters with 1/2 in. of lithium metal, which is contained in a double walled aluminum can.

CHAPTER 3

RESULTS AND DISCUSSION

Tables 4, 5, and 6 show the fast neutron flux versus
distance relations, spectra, and neutron and gamma dose
versus distance relations for 4 different distances from the
center of the reactor. The data have been normalized
arbitrarily to a kw-sec base. The thermal neutron data as
a function of distance are shown in Table 7.

The neutron flux and tissue dose spectral evaluations
indicate softer spectra than those observed with the Godiva II
assembly (6). The measured gamma to neutron dose ratio is
the lowest observed ($\sim$ 3 per cent) at any critical assembly
tested thus far. These comparisons are shown in Table 8.

The estimated uncertainties for the tissue dose measure-
ments are approximately 15 per cent, whereas the uncertainties
in the gamma measurements are somewhat higher (25 per cent)
due to the low gamma to neutron dose ratio observed and the
fast neutron response factor.

TABLE 4. NEUTRON FLUX VERSUS DISTANCE RELATIONS FOR THE LITTLE EVA CRITICAL
ASSEMBLY

Distance from Center, cm	$n/cm^2/kw-sec \times 10^8$			
	Pu^{239} $E_n > 0.004$ Mev	Np^{237} $E_n > 0.75$ Mev	U^{238} $E_n > 1.5$ Mev	S^{32} $E_n > 2.5$ Mev
50	22.6	7.42	3.80	1.51
75	8.45	3.50	1.60	0.682
100	4.57	1.68	0.753	0.298
150	3.02	1.19	0.377	0.168

TABLE 5.   NEUTRON FLUX AND TISSUE DOSE SPECTRAL EVALUATIONS[*]
FOR THE LITTLE EVA CRITICAL ASSEMBLY

Energy Interval, Mev	Neutrons, per cent	Tissue Dose, per cent
0.004 - 0.75	62	43
0.75 - 1.5	22	28
1.5 - 2.5	9	15
>2.5	7	14

[*]Average of data in Table 4.

TABLE 6.   NEUTRON AND GAMMA DOSE VERSUS DISTANCE RELATIONS
FOR THE LITTLE EVA CRITICAL ASSEMBLY

Distance from Center, cm	Neutron Tissue Dose, rads/kw-sec	Gamma Dose, roentgens/kw-sec
50	3.90	0.094
75	1.64	0.020[*]
100	0.838	0.025
150	0.550	0.010[**]

[*]Low value.
[**]Interpolated data.

TABLE 7.   THERMAL NEUTRON FLUX VERSUS DISTANCE RELATIONS
FOR THE LITTLE EVA CRITICAL ASSEMBLY

Distance from Center, cm	Thermal Neutron Flux, $E_n < 0.5$ ev $n/cm^2 \times 10^7$/kw-sec	Cadmium Ratio[*]
50	2.35	2.2
75	2.60	2.6
100	2.28	3.0
150	2.03	2.7

[*]Defined as $\dfrac{\text{bare gold activity/mass}}{\text{cadmium covered gold activity/mass}}$

TABLE 8. COMPARISON OF LITTLE EVA AND GODIVA II NEUTRON FLUX AND TISSUE DOSE SPECTRA

Energy Interval, Mev	Neutrons in Energy Interval, per cent		Tissue Dose in Energy Interval, per cent		Dose Ratio, $\dfrac{\text{Gamma (r)}}{\text{Neutron (rads)}}$	
	Little Eva	Godiva II	Little Eva	Godiva II	Little Eva	Godiva II
0.004 – 0.75	62	43	43	24		
0.75 – 1.5	22	22	28	24		
1.5 – 2.5	9	17	15	21	0.03	0.12[*]
>2.5	7	18	14	30		

[*]An average of 3 different methods of measurement: graphite-CO_2 ionization chamber (5), 0.09; tetrachloroethylene chemical dosimeters (7), 0.15; and hexafluorobenzene plus 9,10-diphenylanthracene organic scintillator (8), 0.12.

REFERENCES

(1)   Young, D. S., Los Alamos Scientific Laboratory Report LA-1487 (May 1952).

(2)   Hurst, G. S., J. A. Harter, P. N. Hensley, W. A. Mills, M. Slater, and P. W. Reinhardt, Rev. Sci. Instr. <u>27</u>, 153 (1956).

(3)   Reinhardt, P. W. and F. J. Davis, Health Phys. <u>1</u>, 169 (1958).

(4)   Hurst, G. S. and R. H. Ritchie, Oak Ridge National Laboratory Report ORNL-2748, Part A (November 1959).

(5)   Sayeg, J. A., E. R. Ballinger, and P. S. Harris, Los Alamos Scientific Laboratory Report LA-2310 (March 1959).

(6)   Sayeg, J. A., Los Alamos Scientific Laboratory Report LA-2432 (April 1960).

(7)   Ott, D. G., Los Alamos Scientific Laboratory Report LA-2249 (August 1958).

(8)   Williams, D. L. and F. N. Hayes, Los Alamos Scientific Laboratory Report LA-2375 (November 1959).